EFFECT OF BALL MILLING ON THE MAGNETIC PERFORMANCE OF STRONTIUM FERRITE (SrFe₁₂O₁₉) POWDERS

Oluwasola K. Arigbabowo ¹, Mehadi Hassan ², Azin Asadollahnejad ², Md Shafikul Islam ², Holt Price ², Wilhelmus J Geerts ^{1,3}, Jitendra Tate *,1,2</sup>

Texas State University
601 University Drive, San Marcos, TX,78666

¹Materials Science Engineering and Commercialization Program

²Ingram School of Engineering

³Department of Physics

ABSTRACT

The primary advantage of the high energy ball milling (HEBM) process is its ability to synthesize a homogeneous mixture with submicron (up to nanoscale) particle size. This approach is a viable process for particle size reduction and grain refinement of magnetic powders, which affects their domain structure and by extension the resulting magnetic properties. In this research, we designed a 9-ball milling experiment by keeping the rotational speed constant at 300rpm and varying the ball-to-powder ratio of 5:1, 8:1, and 10:1 for 6hrs, 10hrs, and 14hrs milling times. The strontium ferrite magnetic powders subjected to HEBM were analyzed for crystallite size and behavior via XRD, particle size reduction via SEM/ImageJ software/originLabPro, and magnetic performance via powder-based VSM measurement. The magnetic performance of the ball-milled strontium ferrite powders shows a good combination of appreciable increment in the S-values (a ratio of the remanence to saturation magnetization) and a considerable decline in coercivity (<10% decrease) at 6hrs of milling duration. The particle size obtained at 6hr-8:1BPR is 0.59 µm with about 44% reduction from the 1.05 µm particle size of the unmilled strontium ferrites, which is within the reported single-domain particle critical size (0.5 μ m – 0.65 μ m). The particle size reduction of 0.59 µm at 6hr-8:1BPR would be beneficial in enabling strong interfacial bonding when the ballmilled strontium ferrite powders are used in polymer-bonded magnets.

Keywords: Strontium ferrite, High Energy Ball Milling, Milling Parameters, Magnetic domain structure – single and complex, Vibrating Sample Magnetometer

Corresponding author: Dr. Jitendra S. Tate

*Email: jt31@txstate.edu, Phone: (737) 262-8010

Copyright 2024. Used by the Society of the Advancement of Material and Process Engineering with permission.

SAMPE Conference Proceedings. Long Beach, CA, May 20-23, 2024. Society for the Advancement of Material and Process Engineering – North America.

(https://doi.org/10.33599/nasampe/s.24.0161)

1. INTRODUCTION

The global appeal of ferrite magnetic powders as technological alternatives for permanent magnetic materials stems from their affordability, chemical inertness and stability, low toxicity, high Curie temperature, and appreciable magnetic properties [1]. Specifically, the hexagonal M-type ferrites such as strontium ferrite (SrFe₁₂O₁₉), are a versatile permanent magnetic material that has received significant attention in various applications such as magnetic recording media and permanent magnetic motors [2]. The hexagonal M-type strontium ferrites magnetic powders exhibit hexagonal crystal, and its magnetic anisotropy behavior can be attributed to its unique crystal structure where the basal plane is the hard direction for the magnetic dipole moment and its easy axis of magnetization is along the c-direction of the hexagonal crystal structure. Such crystal magnetic anisotropy behavior enables the optimization of magnetic properties such as the remanent magnetization, or coercive field, which are strongly dependent on the microstructure, sintered density, and particle sizes of the strontium ferrite magnetic powders [3].

Particle size reduction of magnetic materials to the nanoscale has been identified as a viable means of preventing multi-domain structures and facilitating single-domain structures required to increase the coercive field of magnetic materials. These magnetic domains are regions within a magnetic material where the magnetic moments of atoms align in the same direction. In single-domain regions, all the magnetic moments are uniformly aligned, creating a strong, resultant magnetic field. Single magnetic domains exhibit strong ferromagnetic behavior and have a net magnetic moment even without an external magnetic field. In order to achieve these single-domain nanostructured magnetic materials, wet chemical synthesis techniques such as co-precipitation [4], hydrothermal [5], sol-gel [6], and microemulsion [7] synthesis techniques have been widely reported. However, these techniques are not eco-friendly because they are solvent-dependent techniques. Alternatively, mechanosynthesis via ball milling techniques has been identified as a more viable option for achieving nanosized magnetic particles with high coercive field and magnetic saturation.

Ball milling techniques are particle size reduction methods that are energy and cost-efficient, scalable, and suitable for the mass production of nanostructure materials [8, 9]. It is a mechanical process for grinding, mixing, and blending materials into fine powders or nanomaterials that involves loading the material and grinding media, rotating the mill, crushing, impacting, and shearing the material, and mixing to create homogeneous blends or alloys [9]. Ball milling reduces particle size in magnetic powder particles, leading to the production of finer magnetic powders that enhance the uniformity and homogeneity of magnetic particles, resulting in improved magnetic properties of the milled magnetic powders [10]. There has been a concerted research effort in employing ball milling techniques to synthesize high-performance magnetic powders.

A. L. Rominiyi et al. [11] investigated the impact of varying milling duration and ball-to-powder weight ratio on the crystallite size and lattice strain of nanocrystalline cobalt powder synthesized via mechanical ball milling. After 12 hours of milling, there was an observable reduction of crystallite sizes from 64.8 nm to 9.05 nm, with an appreciable 3.74 % increase in lattice strain when compared to the unmilled powder's baseline strain level of 0.3%. The significant

reduction in crystallite size and the appreciable increase in lattice strain were primarily attributed to the pronounced influence of lattice defects, including stacking faults, dislocations, and other structural imperfections. These defects stem from the extreme plastic deformation of the powder particles due to the impact interactions experienced between the powder, stainless-steel balls, and the interior wall of the milling vial. The authors reported outstanding results of the lowest crystallite size of 13.73 nm, and the highest lattice strain of 0.79%, which were achievable at an optimal ball-to-powder ratio of 10:1 [11]. Cedeño-Mattei, Y.et al. [12] evaluated the effects of particle size reduction on the coercive field of ball-milled cobalt ferrite using tungsten carbide balls and a constant ball-to-powder ratio of 40:1. The authors reported a size reduction of ballmilled cobalt ferrite powders from 18 nm to 10 nm and a decrease in overall surface area. The coercivity of the 18 nm cobalt ferrite nanocrystals was observed to drop from 4910 Oe to 4506 Oe following a 10-hour milling period, which reduced its size to 10nm. This decrease in coercivity was mostly attributed to the size reduction that occurred during the 10-hour milling process, which started at 18 nm and ended at 10 nm. [12]. Mendoza-Suarez, G., et al. [13] reported the synthesis of Zn-Sn-substituted barium ferrite (BaM) powders through low-energy ball milling, employing a rotational velocity of 92 revolutions per minute (rpm) combined with a powder-to-ball mass ratio of 10:1, and subsequent heat treatment. The grain size reduction reported from this study ranged from 0.2 to 1.0 µm. As finer grain sizes (around 100 nm) are deemed ideal for high-density magnetic recording, the authors emphasized that further investigations, possibly involving highenergy milling, would be ideal to achieve this desired grain refinement. [13]. Nowosielski et al. [14] employed ball milling to synthesize barium ferrite from a stoichiometric proportion of barium carbonate and iron oxide. They investigated the microstructure and magnetic properties analysis of barium ferrite powder synthesized via milling. From the SEM morphology images, it was observed that the particle sizes increase with milling time, however increasing the milling time up to 20 hours enables accumulation of smaller magnetic particles into bigger agglomerates. This was attributed to higher active surface areas associated with the fineness of the magnetic powders [14].

Based on the existing literature with some summarized in the above paragraphs, it can be inferred that high energy ball milling operation is capable of particle size reduction of the hard magnetic ferrite to submicron sizes (up to nanoscale), where the formation of a magnetic multidomain structure can be prevented and a single-domain structure that results in improvement of magnetic properties can be facilitated. By optimizing the milling process parameters such as ball to powder ratio, milling duration and milling rotational speed, adequate size reduction and small size distribution are obtainable. In addition, ball milling operation has been identified as a simple, scalable, and affordable approach for mass production of finer magnetic powders [15]. The specific surface area of such finer magnetic powders can be enhanced by mechanical activation via ball milling, which makes them more reactive for interfacial bonding when used to develop sintered or bonded magnetic composite viable in applications such as 3D-printed Halbach cylinders that can be used in portable, low-frequency MRI equipment for diagnostic imaging in the medical field, magnetic robots made from magnetic nanocomposite for drug delivery in biomedical applications, and permanent bonded magnetic materials exclusively used in the motor systems in electric cars.

Hence, this research aims to investigate the effects of the ball milling process parameters on the magnetic performance of strontium ferrite powders by monitoring how the particle sizes influence their permanent magnetic properties.

2. EXPERIMENTATION

2.1 Materials

The magnetic material subjected to ball milling operation in this study is strontium ferrite, which is trademarked as "OP 56" and supplied by DOWA Electronics. Strontium ferrite is a hexaferrite ceramic material sought after for its affordability, magnetic properties, mechanical strength, thermal stability, and chemical inertness. Strontium ferrite powders are ideal magnetic materials for manufacturing cost-effective magnetic devices with permanent magnetic properties. As stipulated in its technical data sheet (TDS), the as-received strontium ferrite (OP 56) magnetic powders exhibit an average particle diameter (APD) of 0.96 nanometers and were manufactured as magnetic orientation powders. The OP-56 strontium ferrite powders have an excellent combination of crystalline orientation and high coercivity which are critical factors for magnetic performance. **Table 1** highlights the magnetic properties according to the TDS of the as-received OP-56 strontium ferrite powders [16].

Table 1. Materials specification of strontium ferrite powders (OP-56)

Product	APD	* BET	CD	Compression-molded			Bulk Powder	Powder
	μm	SSA M^2/g	g/cm3	Br mT G	HcB kA/m Oe	P-HcJ kA/m Oe	HcJ kA/m Oe	рН
OP-56	0.96	2.88	3.13	191 1910	129 1626	259 3260	300 3765	9.3

2.2 High Energy Ball Milling

Strontium ferrite (OP 56) was subjected to high-energy ball milling operation using an ACROSS planetary high-energy ball mill with model PQ-N04.110 shown in **Figure 1**. It can hold 4 100ml jars and can obtain constant rotation speeds of 0-600 RPM. The planetary high-energy ball mill equipment has the capability of granularity reduction up to 0.1 microns (100 nm) and a maximum milling time of 72 hours.







Figure 1. (a) ACROSS High Energy Ball Mill (b) Planetary system of the ball mill (c) TEFLON grounding jar and ceramic balls.

The high-energy ball milling experiment conducted on the strontium ferrite (OP 56) is summarized in Table 2. After the initial trial run via dry ball milling, it was observed that there was severe heat accumulation and higher internal friction which led to the strontium ferrite attaching to the vial walls and no efficient milling was achieved. Consequently, wet ball milling was adhered to during the milling operation to prevent such heat accumulation that can potentially distort the crystalline structure of the strontium ferrite powder and adversely impact its magnetic properties. For the wet ball milling experiments, distilled water was used as the solvent considering that strontium ferrite powder is very polar and water friendly. The grounding jar used in this experiment is a non-sticky PTFE/TEFLON vial to minimize the agglomeration of these powders to the vial wall and it is also sealed with a silicon gasket to prevent exiting of the grinding media during ball milling. For the ball milling experiment, milling speed was kept constant at 300 rpm, and both the ball-to-powder ratio and milling time were varied. The 3 variations of ball-to-powder ratios (BPR) utilized in this experiment are 5:1, 8:1, and 10:1 at 3 different milling times of 6, 10, and 14 hours making a total of 9 experiments as summarized in **Table 2**. The weight percentage of distilled water used as a solvent for the wet ball milling operation is 100%. This is to ensure slurry grinding media formation instead of suspension, which will enable an adequate impact and shearing forces of the grounding balls on the strontium ferrite powders.

Table 2. High Energy Balling Experiment

Experiment Number	RPM		Time(hours)	Dry or Wet	Powder Weight(g)	Weight of Water
1	300	5 to 1	6	Wet	6.5	100%
2	300	8 to 1	6	Wet	4.1	100%
3	300	10 to 1	6	Wet	3.2	100%
4	300	5 to 1	10	Wet	6.5	100%
5	300	8 to 1	10	Wet	4.1	100%
6	300	10 to 1	10	Wet	3.2	100%
7	300	5 to 1	14	Wet	6.5	100%
8	300	8 to 1	14	Wet	4.1	100%
9	300	10 to 1	14	Wet	3.2	100%

2.3 Materials Characterization

After the ball milling experiment, the received and the milled strontium ferrite magnetic powder (OP 56) was subjected to characterization using X-ray diffraction (XRD) to study their crystallographic state, Scanning Electron Microscopy (SEM) to evaluate the morphology and particle sizes, and Vibrating Sample Magnetometer (VSM) to investigate the effect of milling operation on their magnetic performance.

The XRD study was conducted using advanced Rigaku XRD equipment in Bragg Brentano mode, which is recommended for powdery samples. Sample preparation involved cleaning the glass slide sample holder with isopropyl alcohol (IPA) and nitrogen before introducing the strontium ferrite sample and ensuring we maintained a flat sample surface. The glass slide sample holder has a 3 mm (about 0.12 in) deep square slot on it and an allowable maximum height of 3mm when loaded with a strontium ferrite sample. Before taking the 2-theta measurement of our sample according to the parameters presented in **Table 3**, a 4.5-minute alignment process was carried out to ensure accurate and reliable data. The monochromator is made using the K-β filter method which avoids the chance of any secondary radiation. The crystallite size was determined using the XRD software from the peak width of the peak with the highest intensity in the XRD spectra.

Table 3. XRD parameters for the measurement

Parameters	Measurement
Range of theta, 2-theta	20°-80°
Speed	10°/min
Step	0.01°/min

A scanning electron microscopy study was conducted via a JEOL SEM to evaluate the morphological characteristics and particle size estimation of the ball-milled strontium ferrite powders. Prior to SEM investigation, ball-milled samples were sputter coated using an Imaging Sputter Coater machine to enable good imaging without the electrons charging effects. The samples were coated with a 2nm gold conductive layer to enable electron beam penetration and conduction, thereby eliminating sample charging due to the accumulation of electrons on the non-conductive samples. The parameters used in the SEM study are summarized in **Table 4** below.

Table 4. SEM parameters for the measurement

Parameters	Measurements
Accelerating Voltage	20 Kv
Spot Size	35
Working distance	11-12
Magnification	x9000-x12000

The magnetic properties of the milled powder were analyzed with a MicroSense EZ9 bi-axial Vibrating Sample Magnetometer (VSM) to obtain the hysteresis curve for each of the ball milling experiments. The instrument was calibrated with a 3 mm long 2 mm diameter nickel wire that has

approximately the same shape and size as our powder samples. The magnetic moment of the Ni wire was estimated from its mass (97.227 mg) assuming its magnetic moment per unit of mass is 54.95 emu/gr. A vertical Formolene 4100N Quantum Design powder cup attached to a 3 mm OD Pyrex glass tube inserted in a MicroSense keyed sample rod adapter (see Fig. 2 below) was used as the sample holder. Approximately 22 mg of dried powder was loaded in the powder cup in zero field without matrix material and compacted with a polypropylene stopper. Note that we have no control on the orientation of the particles in the cup holder but expect that most platelets will have their c-axis oriented in the vertical direction. The exact mass of the powder was measured in five significant digits using a Cahn-30 microscale down to 1 microgram. After loading the sample in the VSM the sample-position was centered in between the pick-up coils before starting the hysteresis curve measurement. The field range of the applied magnetic field for the hysteresis curve measurements was between -22000Oe to +22000Oe. Measurements were done in sweep mode using a sweep rate of 400 Oe/s for two different field angles. The raw hysteresis curves were corrected for the image effect and the field lag. The magnetic hysteresis curve obtained from the magnetometry characterization is to evaluate primary magnetic properties - magnetic coercivity, remanent magnetization, and saturation magnetization of each sample powder subjected to wet ball milling.



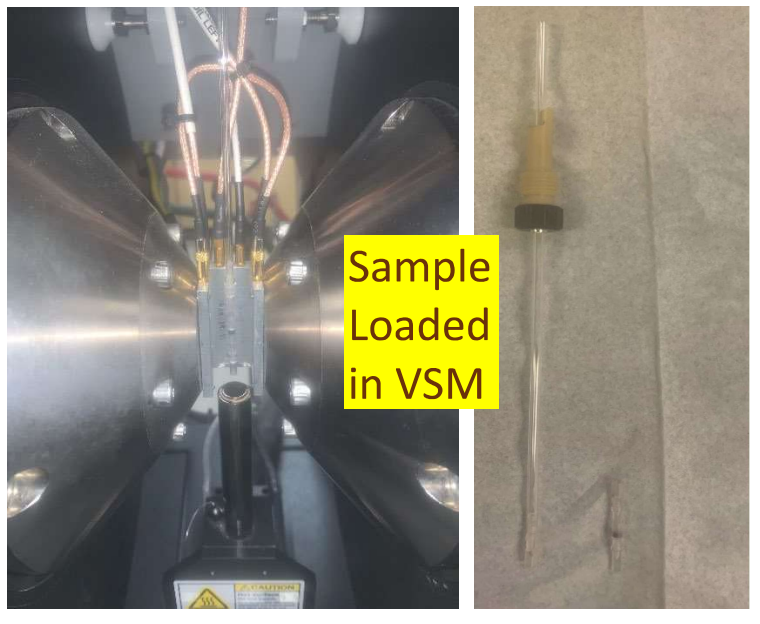


Figure 2. (a) Vibrating Sample Magnetometer (VSM) (b) Sample rod and powder cup (c) sample loaded in the VSM (right).

3. RESULTS AND DISCUSSION

The results obtained from the materials characterization – X-ray Diffraction (XRD), scanning electron microscopy (SEM), and Vibrating Sample Magnetometry (VSM) studies are discussed as follows.

3.1 Crystallite Size and Crystallinity Behavior via XRD.

The average crystallite size obtained from the XRD spectra at different milling times and ball-to-powder ratios is presented in **Figure 3.** According to this figure, it is evident that crystallite sizes were reduced with all different parameters' milling operations compared to the as-received strontium ferrite powders. Over a 6-hour milling period, the average crystallite size is consistently reduced across various ball-to-powder ratio (BPR) ratios. This implies that wet milling effectively breaks down crystalline structures, resulting in smaller crystallite sizes. However, as the milling duration increased to 10 or 14 hours, there was an observable increase in crystallite size, beyond 8:1 ball to powder ratio. This change is attributable to powder agglomeration and cluster formation. Prolonged milling generates particle clustering, which results in the development of bigger entities via interactions, also called cold welding. This clustering phenomenon reverses the prior observed tendency of crystallite size reduction during milling. Hence, milling beyond a certain threshold appears to encourage powder agglomeration, resulting in bigger crystallite sizes.

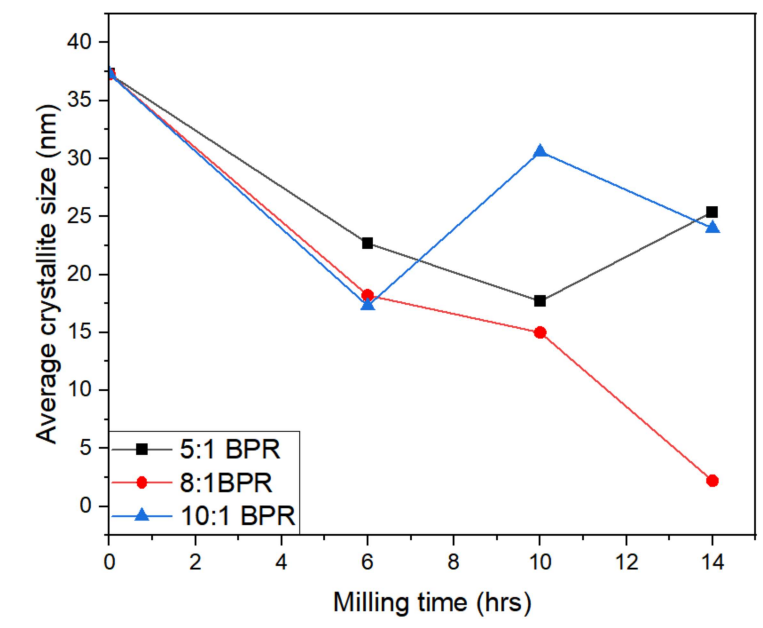


Figure 3. Average crystallite size at different milling times and BPR.

The 2-theta X-ray diffraction peaks obtained for 6 hours milling duration at different ball to powder ratio (BPR) - 5:1, 8:1 and 10:1 BPR is presented in **Figure 4**. According to this figure, there was a noticeable peak broadening at 10:1 BPR after 6 hours of milling, which is evident in all significant planes with highest intensities, such as (008), (107), and (114). The XRD patterns observed are consistent with the work of Stingaciu et al. [17] where the peak broadening was attributed to decrease in crystallite size. These smaller crystallites correspond to wider peaks, which suggests that the milling process actively breaks down crystalline formations into smaller into more defined crystallites.

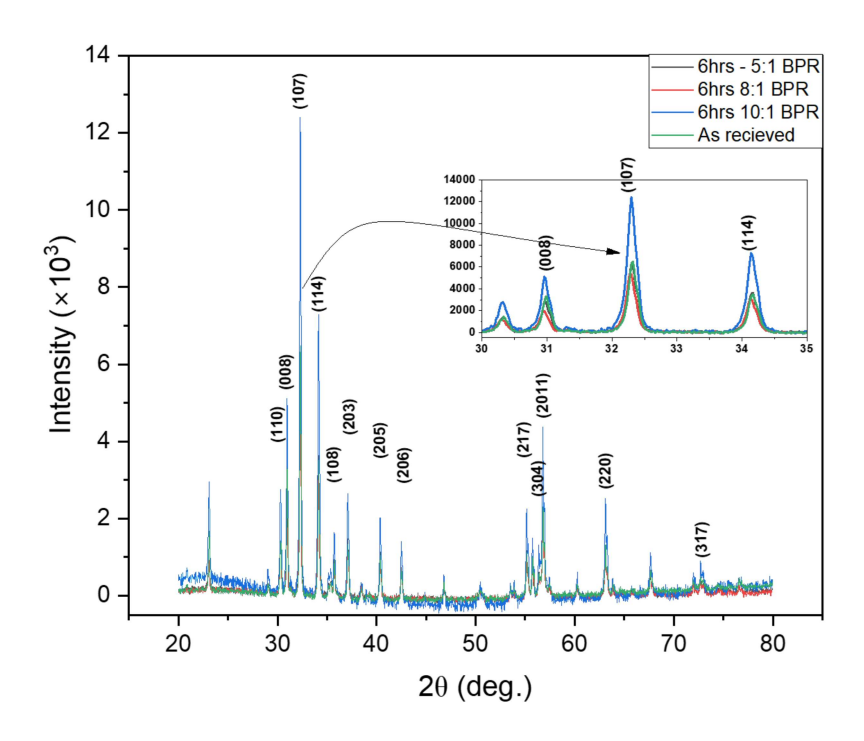


Figure 4. Phase diagram at 6 hours of milling time and different powder ratio

Figure 5 displayed a 2theta XRD pattern for a 10-hour milling time at different ball-to-powder ratios. The XRD peaks have similar intensities with no substantial difference, however, it could be observed that the positions of the crystallite phases have shifted slightly, especially at a 10:1 ball-to-powder ratio. This peak shift is an indication that some modest changes in crystal lattice properties or orientations occurred over an extended 10-hour milling time. Cold welding during the milling process explains the observed peak broadening and phase shifts. Cold welding causes cluster formation by agglomerating powders, increasing crystallite size. This explains why there was an increase in crystallite size at 10 hours at the maximum 10:1 ball-to-powder ratio shown in **Figure 5**.

The XRD pattern shown in **Figure 6** is for 14 hours of milling at different ball-to-powder ratios. It could be observed that there is a slight decrease in peak intensities as shown in (107) and (008) crystallographic planes at a higher ball-to-powder ratio. This is an indication of growing crystallites which can be attributed to some sort of agglomeration. This explains the increase in crystallite size beyond the 8:1 ball to powder ratio at a longer milling time of 14 hours as shown in **Figure 3.** The increase in crystallite sizes observed at longer milling times of 10 and 14 hours at 10:1 ball-to-powder ratio is not unexpected. There is a higher tendency of agglomeration of very small crystallites at such longer milling times because of higher surface energy between the crystallites, thereby enabling their agglomeration and consequently increasing the crystallite sizes.

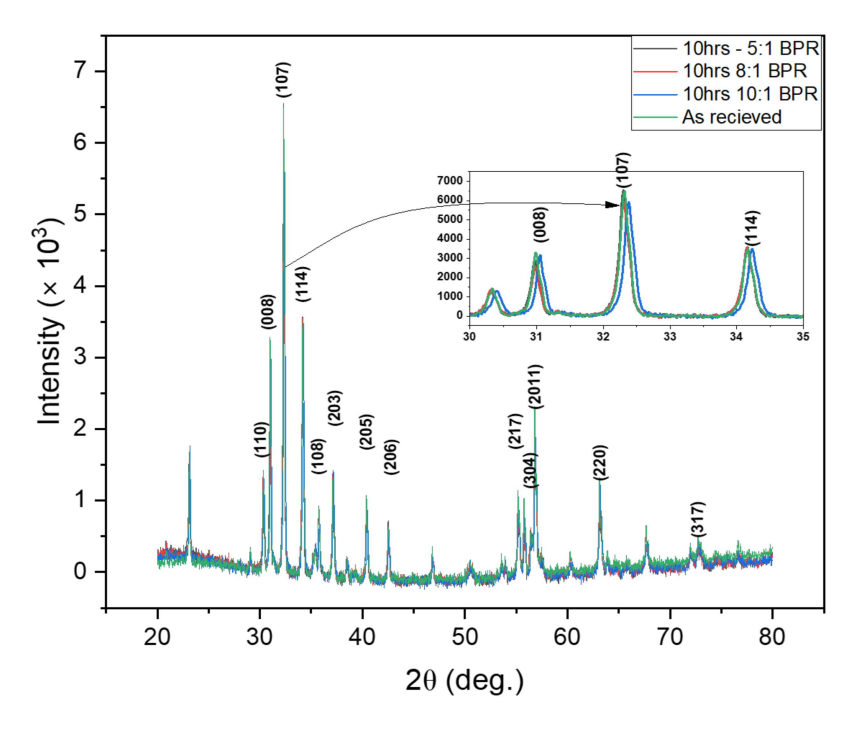


Figure 5. Phase diagram at 10 hours of milling time and different BPR

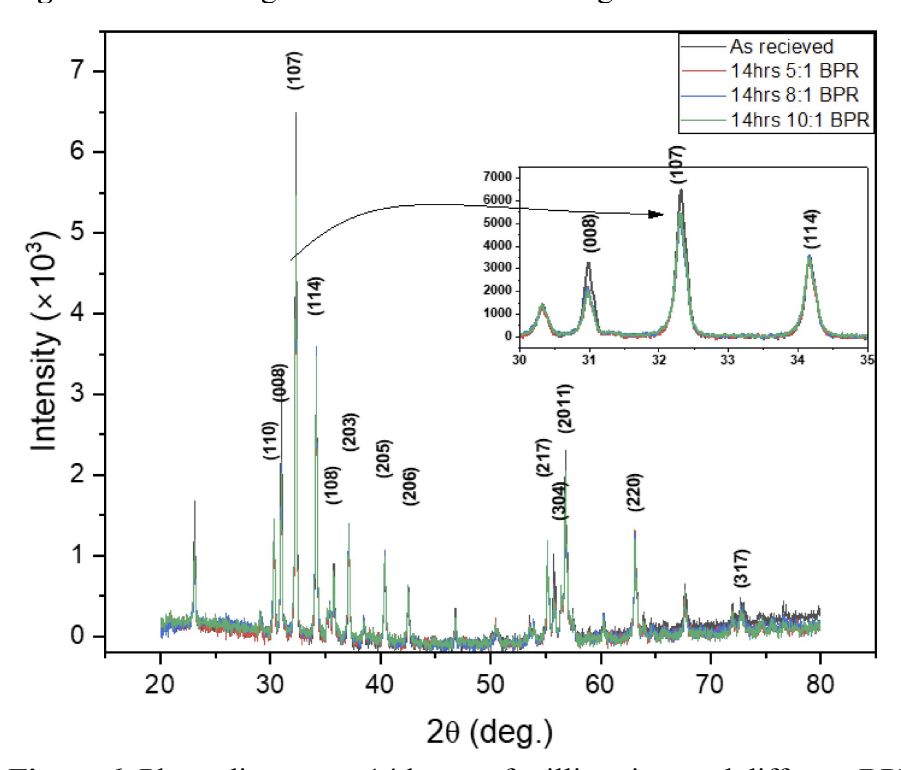


Figure 6. Phase diagram at 14 hours of milling time and different BPR

3.2 Particle Size Evaluation via SEM

The particle sizes of the strontium ferrite magnetic material subjected to ball milling were evaluated via a scanning electron microscope (SEM) and the SEM images obtained were analyzed using Image J software, by counting the individual particle sizes and evaluating an average particle size of the strontium ferrite particles for each ball milling experiment. The image J particle size analysis data was visualized and presented as histograms using originPro software. The SEM images and the histograms obtained from the image J analysis are presented from **Figure 7** to **Figure 10** for the as-received sample and ball-milled strontium ferrites. Additionally, descriptive statistics were run on the image J analysis as presented in **Table 4** to evaluate the central tendency, dispersion, and the shape of the distribution of the image J analysis dataset. The SEM images suggest that the strontium ferrites particles exhibit a platelet morphology.

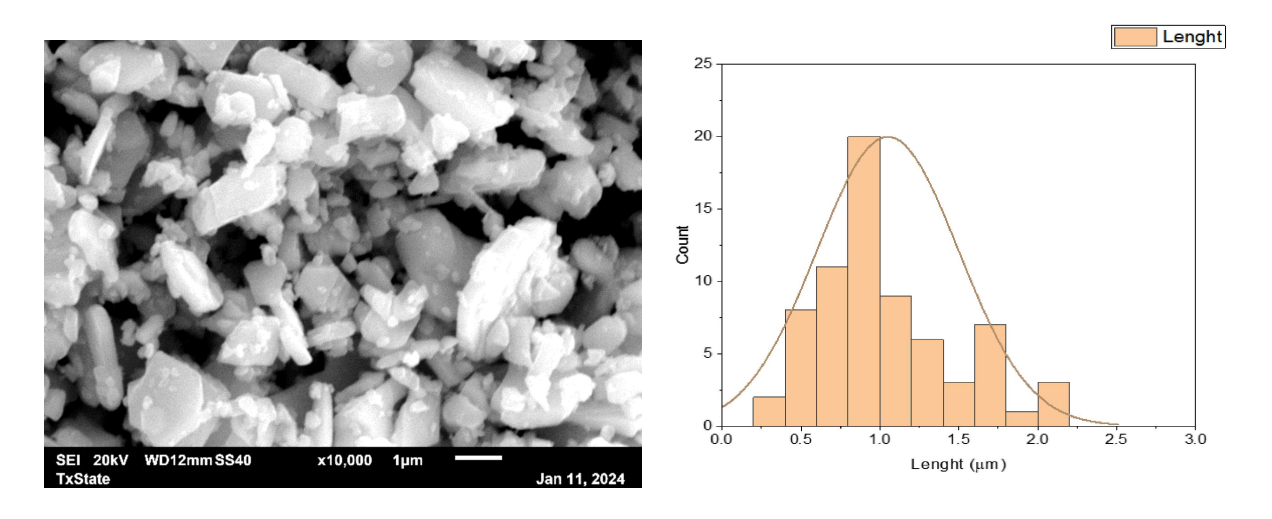
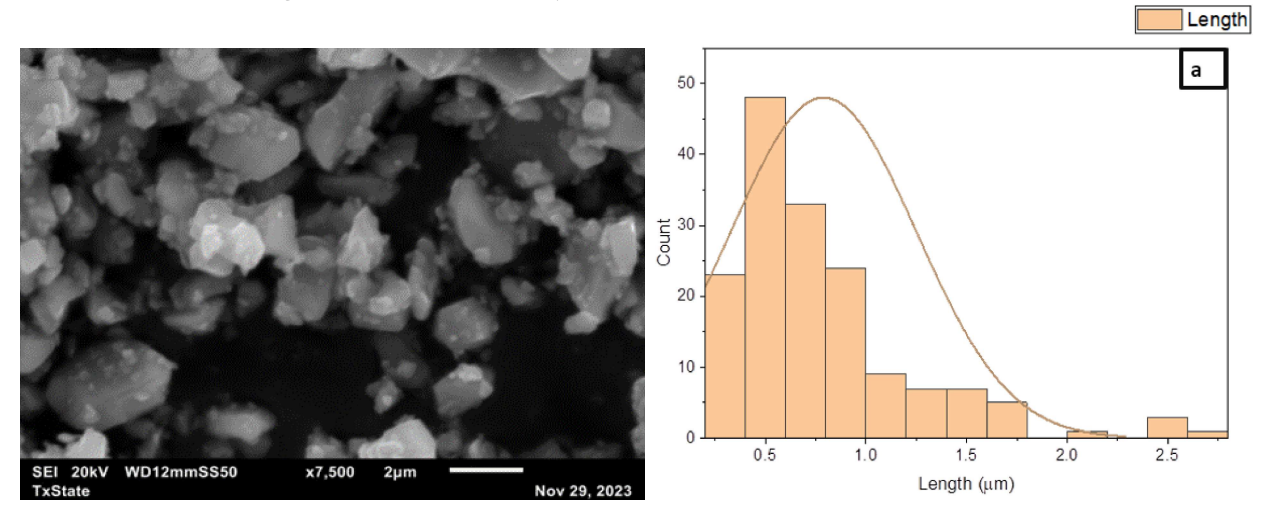


Figure 7. SEM images (left) and particle size distribution (right) for the as-received strontium ferrite powder; average particle size: 1.05 μm.



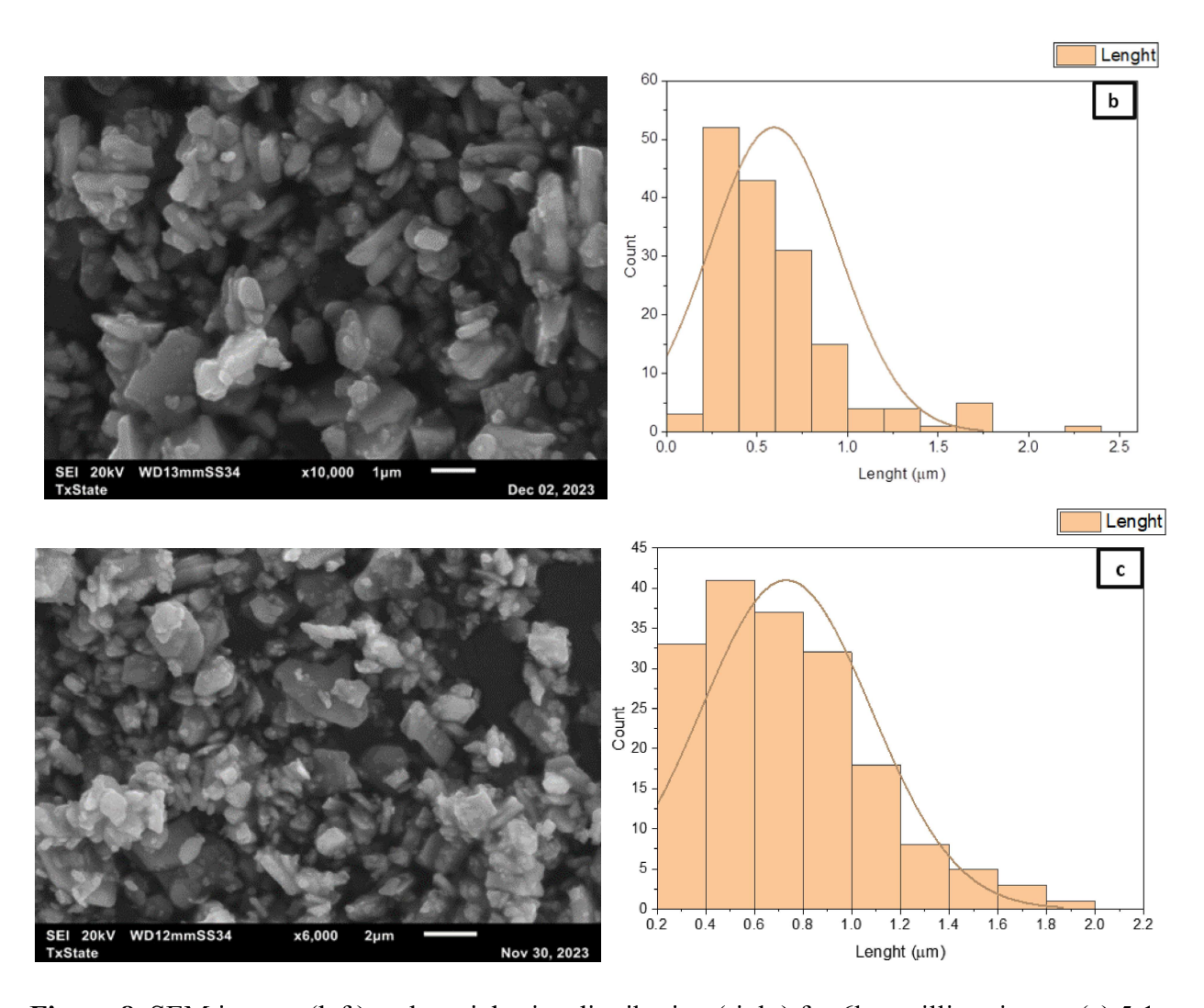
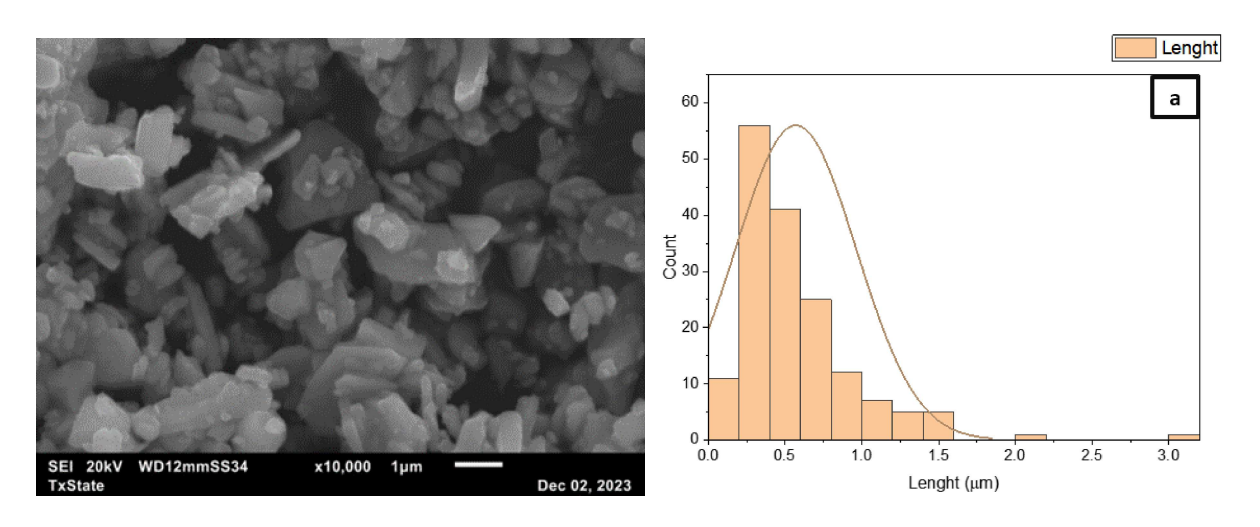


Figure 8. SEM images (left) and particle size distribution (right) for 6hrs milling time at (a) 5:1 (b) 8:1 APD = (c) 10:1 APD = ball to powder ratios (BPR)



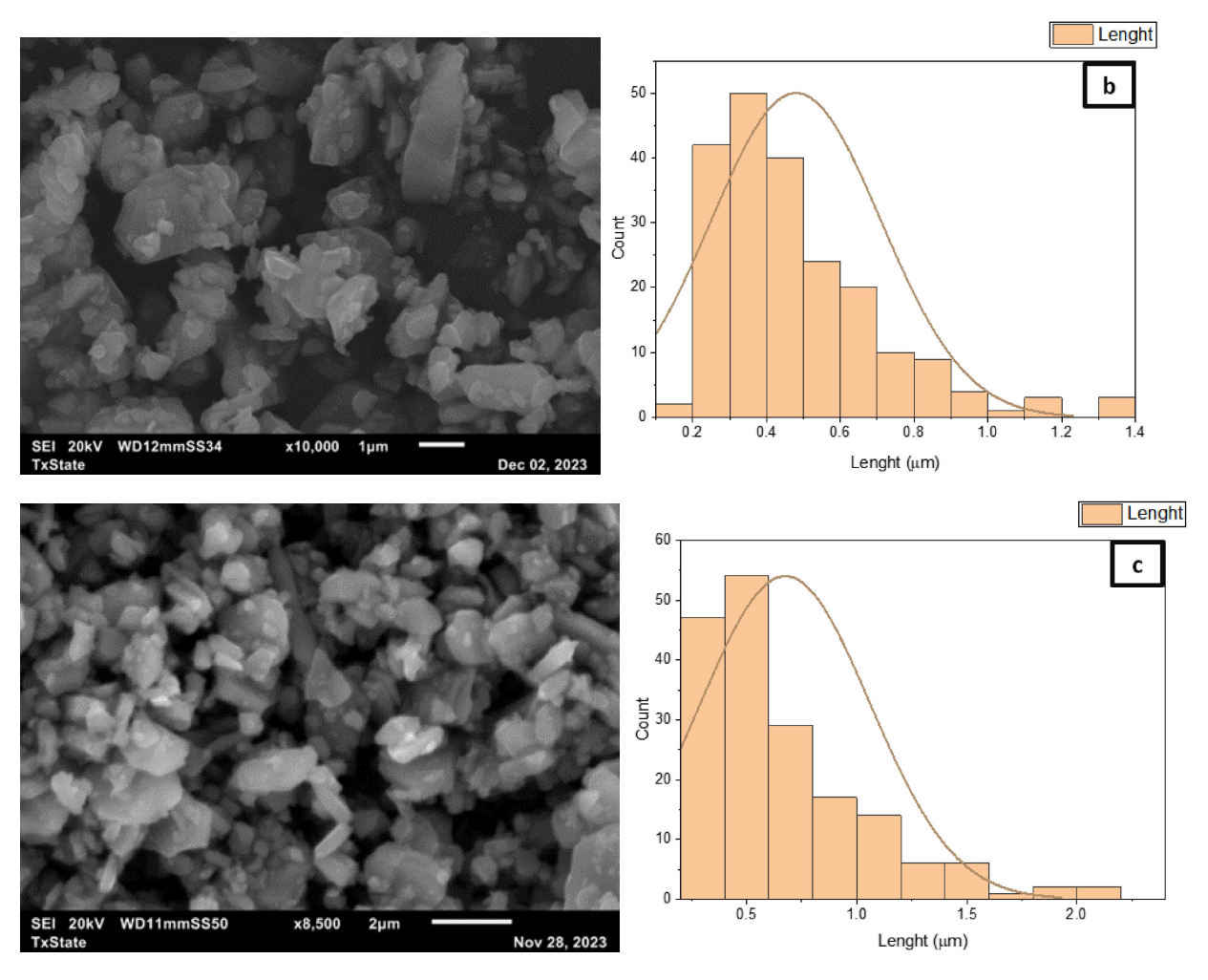
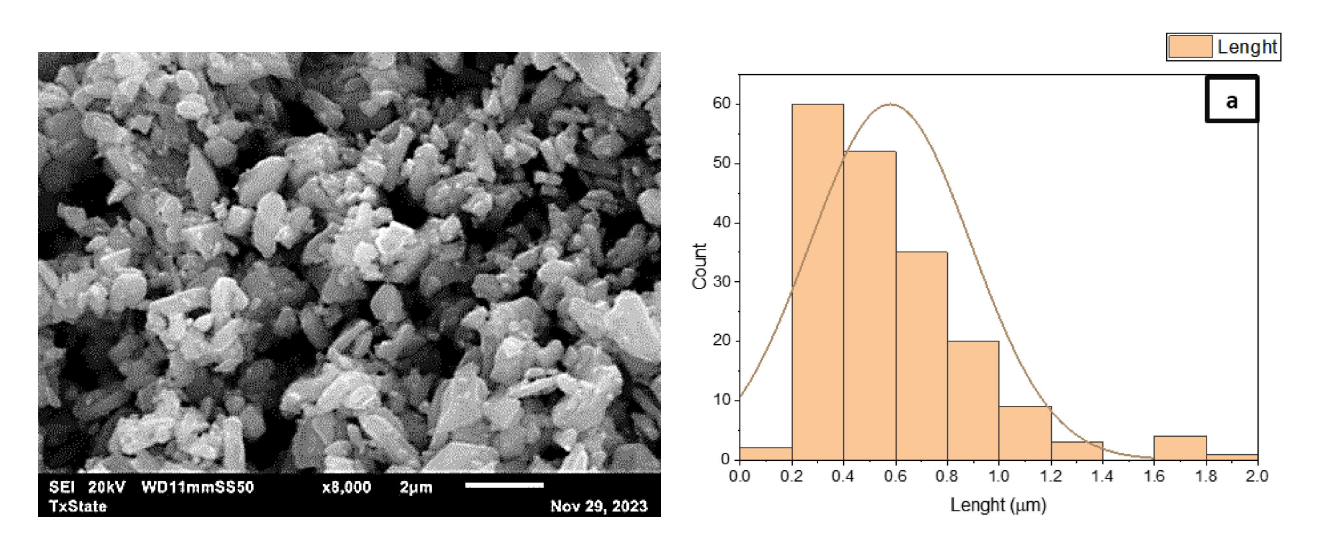


Figure 9. SEM images (left) and particle size distribution (right) for 10hrs milling time at (a) 5:1 BPR (b) 8:1 (c) 10:1 ball to powder ratio (BPR)



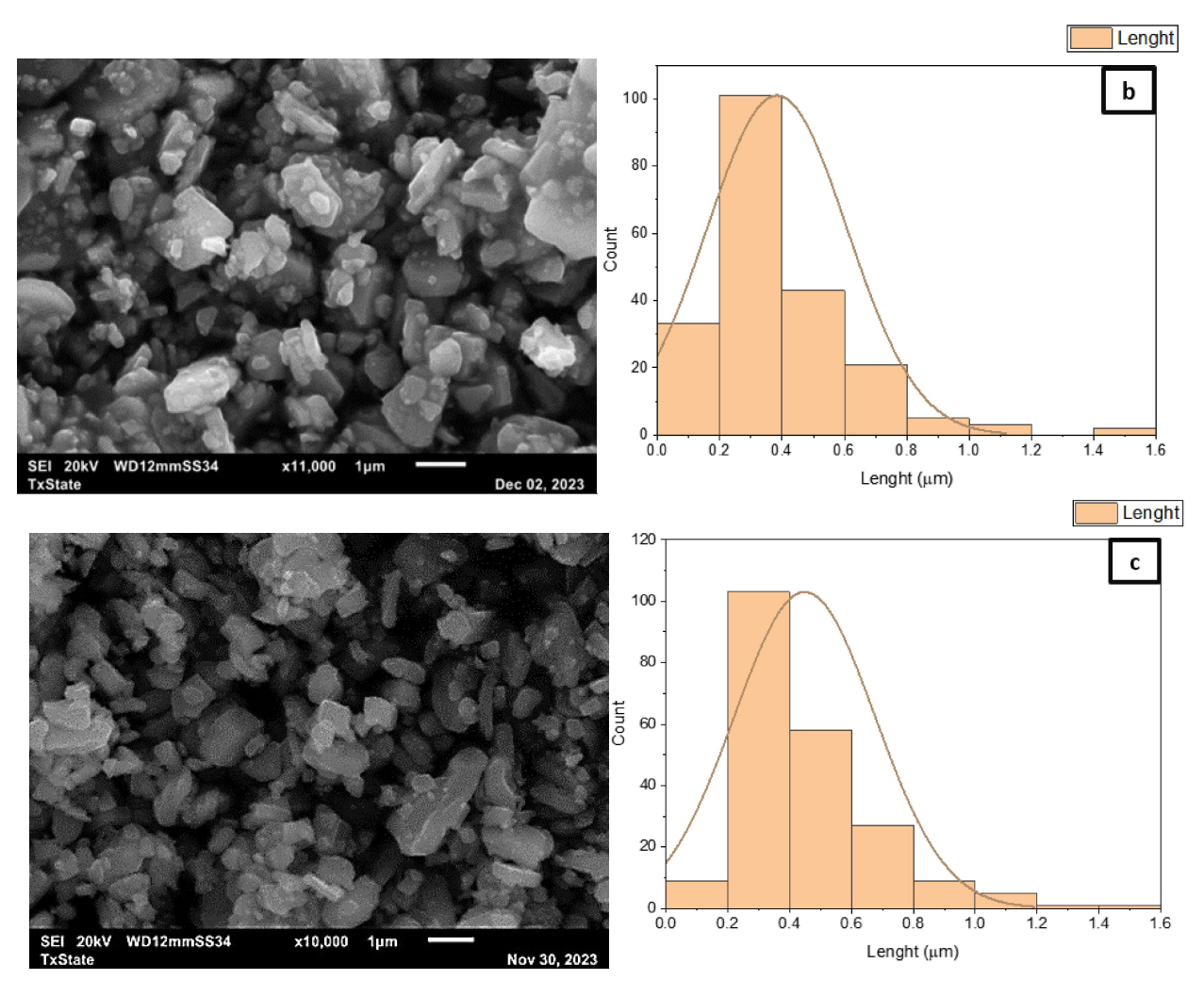


Figure 10. SEM images (left) and particle size distribution (right) for 14hrs milling time at (a) 5:1 (b) 8:1 (c) 10:1 ball to powder ratios (BPR)

Table 4. Descriptive analysis of particle size distribution for each ball milling experiment.

					Standard			
Data	Mean	Min	Median	Max	Deviation	Variance	Sum	N total
14hr 10-1	0.52339	0.183	0.427	1.386	0.27296	0.07451	80.078	153
14hr 8-1	0.38336	0.11	0.3205	1.535	0.22543	0.050082	79.738	208
14hr 5-1	0.57965	0.19	0.4985	1.878	0.31172	0.09717	107.814	186
10hr 10-1	0.67494	0.246	0.5435	2.186	0.38489	0.14814	120.14	178
10hr 8-1	0.47993	0.167	0.428	1.369	0.22964	0.05273	100.3059	209
10hr 5-1	0.57032	0.121	0.435	3.056	0.39359	0.15492	93.532	164
6hr 10-1	0.73087	0.233	0.675	1.999	0.34874	0.12162	130.8249	179
6hr 8-1	0.59318	0.144	0.491	2.203	0.35438	0.12559	94.90818	160
6hr 5-1	0.78927	0.254	0.687	2.622	0.45975	0.21137	127.8623	162
As received	1.05009	0.277	0.9195	2.175	0.44882	0.20144	73.506	70

By analyzing the SEM images, the effect of varying process parameters of the ball milling experiment on strontium ferrites average particle sizes (mean size) was correlated and summarized in **Figure 11**. According to this figure, it is evident that the 8:1 ball-to-powder ratio appears to be more effective in reducing the particle size of strontium ferrite significantly across all milling time, with the largest reduction at 14 hrs. milling time reaching the lowest value of 0.38 μ m. However, there are appreciable (some significant) particle size reductions across all the 9-ball milling experiments, it is noteworthy that the optimal and best combination of milling time and powder-to-ball ratio will be dependent on how this particle size reduction affects the magnetic performance of the ball milled strontium ferrite particles.

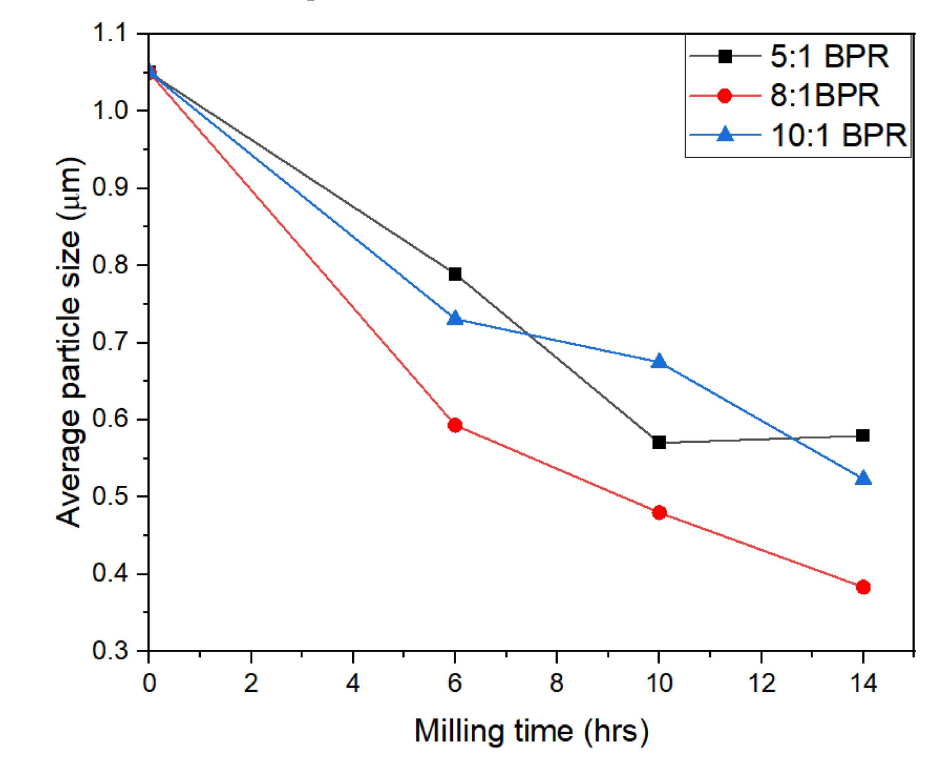


Figure 11. Effect of milling time and ball-to-powder ratio on the average particle sizes of the milled strontium ferrite powders.

3.3 Magnetic properties evaluation via VSM

The magnetic properties data of the as-received strontium ferrites powders and those subjected to wet ball milling were obtained using the vibrating sample magnetometry. This was done by analyzing the obtained magnetic hysteresis loop presented in **Figure 12** for the primary magnetic properties – saturation magnetization, remanent magnetization, and coercive field. The magnetic hysteresis loop is induced magnetization measured as the magnetic moment in emu as a function of the applied magnetic field from -2.2 T to +2.2 T. As shown in **Figure 12**, the maximum magnetic moment induced by the sample under investigation represents the saturation (Ms). The amount of the magnetic moment (induced magnetization) remaining when the applied magnetic field reverts to 0 is the remanence (Mr) of the measured sample. The coercive field, also known as coercivity (Hc) is the amount of applied magnetic field required to reverse the induced magnetization to zero.

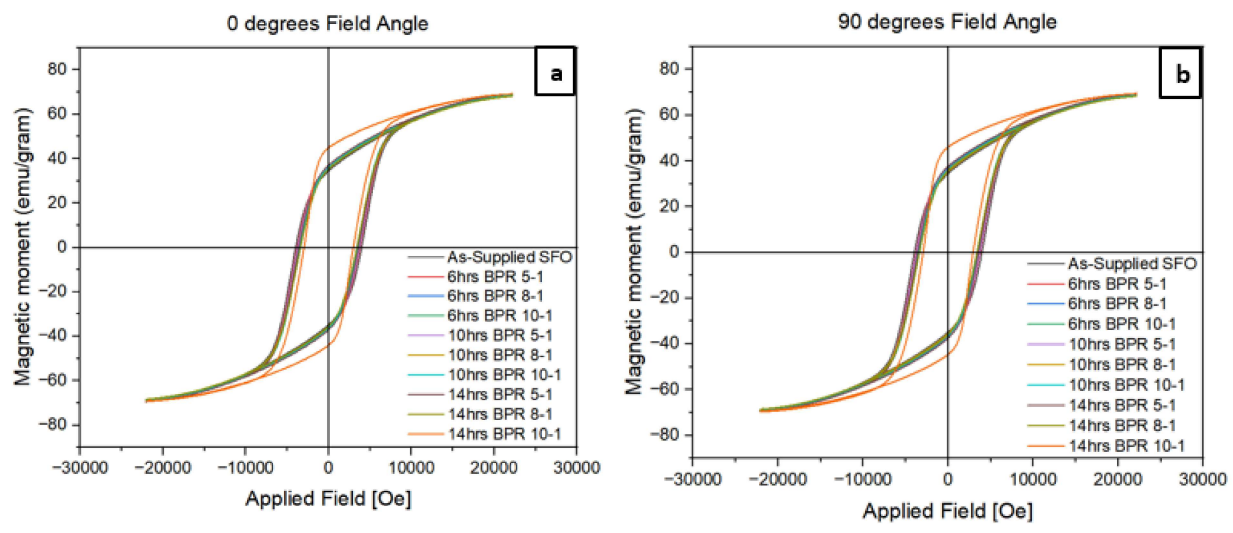


Figure 12. Magnetic hysteresis loops of ball-milled strontium ferrite powders at (a) 0 degrees Field Angle (b) 90 degrees Field Angle

According to **Figure 12**, the magnetic hysteresis loops for the ball-milled strontium ferrite powder obtained at both 0 and 90-degree field angles are consistently similar. Therefore we only considered the 0 degrees Field Angle to extrapolate the primary magnetic properties (Ms, Mr, and Hc), and their values are summarized in **Table 5** for 6hr, 10hr, and 14hrs milling time at 5:1, 8:1, and 10:1 ball-to-powder ratios (BPR) respectively. In order to monitor the trend and evaluate the effects of the milling parameters on the magnetic properties of the milled strontium ferrite powders, the values shown in **Table 5** were visually represented in **Figure 13**.

Table 5. Coercivity, remanent, and saturation magnetization at different milling times.

	6 hr. milling time			10 hr. milling time			14 hr. milling time		
BPR	5 to 1	8 to 1	10 to 1	5 to 1	8 to 1	10 to 1	5 to 1	8 to 1	10 to 1
Mr(emu/g)	36.401	36.717	35.597	36.495	35.411	36.109	37.086	35.549	44.491
Ms(emu/g)	69.897	69.076	69.163	69.370	68.969	69.119	69.442	68.378	69.384
Hc [Oe]	3819.42	3662.34	3573.44	3732.42	3541.18	3447.27	3598.05	3388.46	2977.29

Figure 13 illustrates the effect of the ball milling parameters on the magnetic hysteresis curve squareness (S-values) and magnetic coercivity (Hc). It is noteworthy that we did not have a large control over the orientation of the strontium ferrite platelets in the sample holder during the loading process of the VSM hysteresis measurement, however, the S values and Hc measured at 0 and 90 degrees are the same suggesting that our measured samples are azimuthally symmetrical, and no significant azimuthal anisotropy was introduced. The S-values are an important permanent magnetic parameter that explains the magnetic anisotropy behavior of the magnetic powder and an indication of the degree of magnetic moments alignment. The S-values are obtained as a ratio of the magnetic remanence to magnetic saturations (Mr/Ms), and it's more representative than Mr and Ms since it is a dimensionless parameter and not influenced by factors such as mass or volume

of the investigated sample. The S values of the milled strontium ferrite were observed to increase across all the ball milling parameters combination, and the most significant enhancement was observed at 14hrs 10:1 BPR. This increment in the S-values across the ball milling parameters suggests an enhancement in the remanence (Mr) value, which is a permanent magnetic property of the strontium ferrite powders, and the effect of the ball-milling operation on the saturation Ms was observed to be less than 1 %. The coercive field (Hc) required to demagnetize or revert the induced magnetization to zero was observed to decrease for ball milling parameters with the most substantial decrease observed at 10:1 ball-to-powder ratio across all milling times but most significant at 14hrs. The decrease in the coercive field has been traced to a decrease in shape anisotropy induced at longer milling times [17]. Gu et al. [18] experimentally observed and reported that the exceptional coercivity in strontium ferrite nanofibers was due to a large lengthto-depth ratio of the nanofibers. In another study by Fang et al. [19], the coercivity was ascribed to be dependent on both the size and shape of the magnetic particles, where the smaller the grain size, the stronger the grain boundaries pinning effect on magnetic domains, thereby enhancing the coercive force required to demagnetize the magnetic particles [20]. However, the decrease in shape anisotropy is the more prevalent contributing factor for the decline in coercivity of the milled strontium ferrite in this study, considering its platelets morphology exhibits a lower aspect ratio as suggested in the work of Stingaciulet al. [17] when compared to strontium ferrite nanofibers. This corroborates existing research that both the morphology (shape) and particle sizes dictate the resulting magnetic performance of strontium ferrites.

Considering the ball milling parameters used in this study, it is evident that the 6hrs milling time, 8:1 BPR yielded a good combination of magnetic properties in terms of appreciable S-values (an indication of higher remanence) and a considerable decline in coercivity with a particle size reduction of 0.59 μ m which is within the critical size of a single-domain particle range of 0.5 μ m - 0.65 μ m reported in the literature [18, 21, 22]. Despite that the largest particle size reduction of 0.38 μ m was achievable at 14hr milling time, the coercivity drastically declined which was evident at 10:1 BPR. This decline can be attributed to the agglomeration tendency of the high surface energy individual particles induced by longer milling time, which could develop larger and inhomogeneous grains.

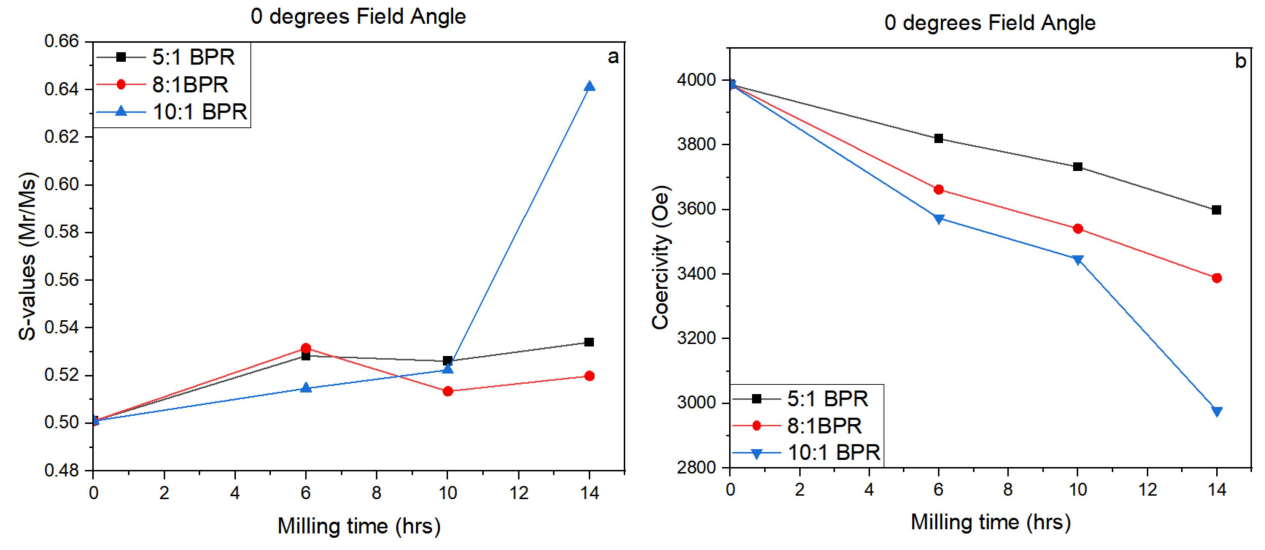


Figure 13. Effects of milling time on magnetic (a) hysteresis squareness (S-values) (b) Coercivity

4. CONCLUSION

Wet ball milling technique using a high energy ball mill (HEBM) was successfully used for particle size reduction of strontium ferrite magnetic powders. The effect of the ball milling parameters on the particle size and by extension the magnetic performance of the strontium ferrite magnetic powders was evaluated.

The X-ray diffraction peaks obtained for the milled magnetic powders showed some peak broadening at 6 hrs. milling time and some decrease in peak intensity at 14hrs. milling time. This suggests some appreciable breaking down of the magnetic particles, resulting in smaller crystallite sizes. The decrease in peak intensities has been ascribed to some agglomeration of extremely small crystallites that may be caused by the higher surface energies of the crystallites. The XRD crystallite size evaluation reveals that the 8:1 ball-to-powder ratio (BPR) appears to be more effective in reducing the particle size of strontium ferrite significantly across all milling time, with the largest reduction recorded at 14 hrs. milling time.

According to the microstructures obtained via scanning electron morphology, there were apparent smaller strontium ferrites platelets at longer milling duration, especially at 14hrs milling time. The smallest particle size evaluated is $0.38 \mu m$, which was obtained at 14hrs, 8:1 ball-to-powder ratio combination. This results in a 64% particle size reduction from $1.05 \mu m$ obtained for the neat (unmilled) strontium ferrite powder.

The coercive field of the milled strontium ferrite was obtained to decrease across all milling parameter combinations. This is peculiar to platelets strontium ferrite magnetic materials. It has been experimentally observed that exceptional coercivity was due to a large aspect ratio (length-to-depth ratio) such as in strontium ferrite nanofibers. The strontium ferrite magnetic powders used in this study exhibit platelet morphology which has a lower aspect ratio compared to nanofibers studied by others and would further be truncated during milling action. This explains the decline in the coercivity observed in this study. An appreciable increase in the S-values (Mr/Ms), which is an important magnetic parameter, was observed across all the ball milling parameters

combination, with the most appreciable enhancement achieved at 14hrs 10:1BPR, however, there was a significant decline in the coercivity for such longer milling times. Considering the ball milling parameters used in this study, it is evident that the 6hr milling time at either a 5:1 or 8:1 ball-to-powder ratio yielded a good combination of magnetic properties in terms of enhanced S-values and a considerable decline in coercivity (<10% decrease). The particle size obtained at 6hr-8:1BPR is 0.59 μ m with about 44% reduction from the 1.05 μ m particle size of the (unmilled) strontium ferrite powder, which is within the critical size of a single-domain particle range of 0.5 μ m - 0.65 μ m reported in the literature. Such particle size reduction is imperative in enabling a strong interfacial bonding between the strontium ferrite powders and a binder when used to develop polymer-bonded magnets.

5. ACKNOWLEDGEMENT

This work was supported in part by NSF through the DMR-MRI Grant under award 2216440 and in part by the DOD instrumentation grant (78810-W911NF-21-1-0253). The authors are thankful to the staff of Texas State University's Analysis Research Service Center (ARSC) and Advanced Composites Lab (ACL).

6. REFERENCES

- [1] R. C. Pullar, "Hexagonal ferrites: A review of the synthesis, properties, and applications of hexaferrite ceramics," *Progress in Materials Science*, vol. 57, no. 7, pp. 1191-1334, 2012/09/01/2012, doi: https://doi.org/10.1016/j.pmatsci.2012.04.001.
- [2] F. N. Tenorio-González, A. M. Bolarín-Miró, F. Sánchez-De Jesús, P. Vera-Serna, N. Menéndez-González, and J. Sánchez-Marcos, "Crystal structure and magnetic properties of high Mn-doped strontium hexaferrite," *Journal of Alloys and Compounds*, vol. 695, pp. 2083-2090, 2017/02/25/ 2017, doi: https://doi.org/10.1016/j.jallcom.2016.11.047.
- [3] A. G. Kolhatkar, A. C. Jamison, D. Litvinov, R. C. Willson, and T. R. Lee, "Tuning the magnetic properties of nanoparticles," *International journal of molecular sciences*, vol. 14, no. 8, pp. 15977-16009, 2013.
- [4] A. Ataie and S. Heshmati-Manesh, "Synthesis of ultra-fine particles of strontium hexaferrite by a modified co-precipitation method," *Journal of the European Ceramic Society*, vol. 21, no. 10, pp. 1951-1955, 2001/01/01/ 2001, doi: https://doi.org/10.1016/S0955-2219(01)00149-2.
- [5] M. Jean, V. Nachbaur, J. Bran, and J.-M. Le Breton, "Synthesis and characterization of SrFe12O19 powder obtained by hydrothermal process," *Journal of Alloys and Compounds*, vol. 496, no. 1, pp. 306-312, 2010/04/30/ 2010, doi: https://doi.org/10.1016/j.jallcom.2010.02.002.
- [6] T. M. H. Dang, V. D. Trinh, D. H. Bui, M. H. Phan, and D. C. Huynh, "Sol-gel hydrothermal synthesis of strontium hexaferrite nanoparticles and the relation between their crystal structure and high coercivity properties," *Advances in Natural Sciences: Nanoscience and Nanotechnology*, vol. 3, no. 2, p. 025015, 2012/05/04 2012, doi: 10.1088/2043-6262/3/2/025015.
- [7] M. M. Hessien, M. M. Rashad, M. S. Hassan, and K. El-Barawy, "Synthesis and magnetic properties of strontium hexaferrite from celestite ore," *Journal of Alloys and Compounds*, vol. 476, no. 1, pp. 373-378, 2009/05/12/ 2009, doi: https://doi.org/10.1016/j.jallcom.2008.08.076.

- [8] M. Cabeza *et al.*, "Effect of high energy ball milling on the morphology, microstructure and properties of nano-sized TiC particle-reinforced 6005A aluminium alloy matrix composite," *Powder Technology*, vol. 321, pp. 31-43, 2017.
- [9] M. Kumar *et al.*, "Ball milling as a mechanochemical technology for fabrication of novel biochar nanomaterials," *Bioresource technology*, vol. 312, p. 123613, 2020.
- [10] W. Xie, E. Polikarpov, J.-P. Choi, M. E. Bowden, K. Sun, and J. Cui, "Effect of ball milling and heat treatment process on MnBi powders magnetic properties," *Journal of Alloys and Compounds*, vol. 680, pp. 1-5, 2016/09/25/ 2016, doi: https://doi.org/10.1016/j.jallcom.2016.04.097.
- [11] A. Rominiyi, M. Shongwe, and B. Babalola, "Development and characterization of nanocrystalline cobalt powder prepared via high energy ball milling process," in *IOP conference series: Materials science and engineering*, 2018, vol. 430, no. 1: IOP Publishing, p. 012029.
- [12] Y. Cedeño-Mattei, O. Perales-Pérez, and O. N. Uwakweh, "Effect of high-energy ball milling time on structural and magnetic properties of nanocrystalline cobalt ferrite powders," *Journal of Magnetism and Magnetic Materials*, vol. 341, pp. 17-24, 2013.
- [13] G. Mendoza-Suarez, K. Johal, H. Mancha-Molinar, J. Escalante-García, and M. Cisneros-Guerrero, "Magnetic properties of Zn-Sn-substituted Ba-ferrite powders prepared by ball milling," *Materials research bulletin*, vol. 36, no. 15, pp. 2597-2603, 2001.
- [14] R. Nowosielski, R. Babilas, G. Dercz, L. Paj¹k, and J. Wrona, "Structure and properties of barium ferrite powders prepared by milling and annealing," *Archives of Materials Science*, vol. 736, p. 736, 2007.
- [15] G. Mendoza-Suarez, J. Matutes-Aquino, J. Escalante-Garcia, H. Mancha-Molinar, D. Rios-Jara, and K. K. Johal, "Magnetic properties and microstructure of Ba-ferrite powders prepared by ball milling," *Journal of magnetism and magnetic materials*, vol. 223, no. 1, pp. 55-62, 2001.
- [16] D. Electronics. "Ferrite powders." https://www.dowa-electronics.co.jp/en/function/ferrite_powder.html (accessed.
- [17] M. Stingaciu, M. Topole, P. McGuiness, and M. Christensen, "Magnetic properties of ball-milled SrFe12O19 particles consolidated by Spark-Plasma Sintering," *Scientific Reports*, vol. 5, no. 1, p. 14112, 2015/09/15 2015, doi: 10.1038/srep14112.
- [18] F. Gu, W. Pan, Q. Liu, and J. Wang, "Electrospun magnetic SrFe12O19 nanofibres with improved hard magnetism," *Journal of Physics D: Applied Physics*, vol. 46, no. 44, p. 445003, 2013.
- [19] L. Fang, T. Zhang, H. Wang, C. Jiang, and J. Liu, "Effect of ball milling process on coercivity of nanocrystalline SmCo5 magnets," *Journal of Magnetism and Magnetic Materials*, vol. 446, pp. 200-205, 2018.
- [20] D. Sellmyer and R. Skomski, Advanced magnetic nanostructures. Springer, 2006.
- [21] S. Ketov, Y. D. Yagodkin, and V. Menushenkov, "Structure and magnetic properties of strontium ferrite anisotropic powder with nanocrystalline structure," *Journal of alloys and compounds*, vol. 509, no. 3, pp. 1065-1068, 2011.
- [22] Z. Zi, Y. Sun, X. Zhu, Z. Yang, and W. Song, "Structural and magnetic properties of SrFe12O19 hexaferrite synthesized by a modified chemical co-precipitation method," *Journal of Magnetism and Magnetic Materials*, vol. 320, no. 21, pp. 2746-2751, 2008.